Computer Methods in Applied Mechanics and Engineering 428 (2024) 117106

Contents lists available at ScienceDirect

Comput. Methods Appl. Mech. Engrg.

journal homepage: www.elsevier.com/locate/cma

Study of the stabilization parameter in the virtual element method

Ryuta Fujimoto [a], Isao Saiki [b,*]

[a] Dia Nippon Engineering Consultants Co., Ltd., Shintoshin 11-2, Chuo-ku, Saitama, 330-6011, Japan
[b] Department of Civil and Environmental Engineering, Tohoku University, Aza-Aoba 6-6-06, Aramaki, Aoba-ku, Sendai, 980-8579, Japan

ARTICLE INFO

Keywords:
Virtual element method
Stabilization parameter
Elasticity
Element stiffness matrix
Eigenvalue analysis
Finite element method

ABSTRACT

The virtual element method is an approximate solution method for partial differential equations that does not require the explicit definition of interpolation functions for test and trial functions in the elements. Accordingly, it can easily handle polygonal and polyhedral elements, including nonconvex shapes, and it has begun to attract attention as a generalization of the finite element method. As one of the two terms that constitute the internal virtual work, the stabilization term has received little attention, and methods for determining the stabilization parameter have not been proposed to date. Thus, in this study, we focus on the stabilization parameter of the stabilization term. Through a series of eigenvalue analyses of the stiffness matrices, we show that the stabilization parameter corresponds to the energy of the mode not included in the consistency term. From this consideration, we propose a method for setting the stabilization parameter appropriately.

1. Introduction

The virtual element method (VEM), proposed by Beirão et al. [1], is an approximate solution method for partial differential equations. Similar to the finite element method (FEM), the VEM discretizes the weak form of partial differential equations using the Galerkin method. However, unlike the FEM, the VEM does not require the explicit definition of interpolation functions within the elements, allowing it to handle arbitrary polygons and polyhedra elements.

Consequently, the VEM has gained attention as a generalization of the FEM. In fact, within less than a decade since the proposal of the VEM theory, it has been applied to various problems. Beirão et al. [2] developed the VEM for two-dimensional linear elastic problems, and Gain et al. [3] extended the theory to three-dimensional problems. In addition, Chi et al. [4] applied the VEM to the finite deformation theory, and Artioli et al. [5] developed nonelastic problems using the VEM. Furthermore, the application of the VEM has been extended to problems, such as topology optimization [6], contact analysis [7], and fracture analysis [8].

As shown in Section 2, the internal virtual work of the VEM comprises two terms: the consistent term and the stabilization term. In particular, the stabilization term is commonly scaled using a stabilization parameter. However, although studies have attempted to tune the stabilization parameter from the mathematical viewpoint [9–13], appropriate methods for tuning the stabilization parameter from the physical and practical aspects have not been established. Therefore, in this study, focusing on two-dimensional linear elastic problems, we clarify the physical significance of the consistency and stabilization terms in the virtual element stiffness matrix for four-node quadrilateral elements through eigenvalue analysis. In addition, we propose a methodology for determining the optimal stabilization parameters.

* Corresponding author.
E-mail address: isao.saiki.a4@tohoku.ac.jp (I. Saiki).

https://doi.org/10.1016/j.cma.2024.117106
Received 14 March 2024; Received in revised form 8 May 2024; Accepted 29 May 2024
Available online 7 June 2024

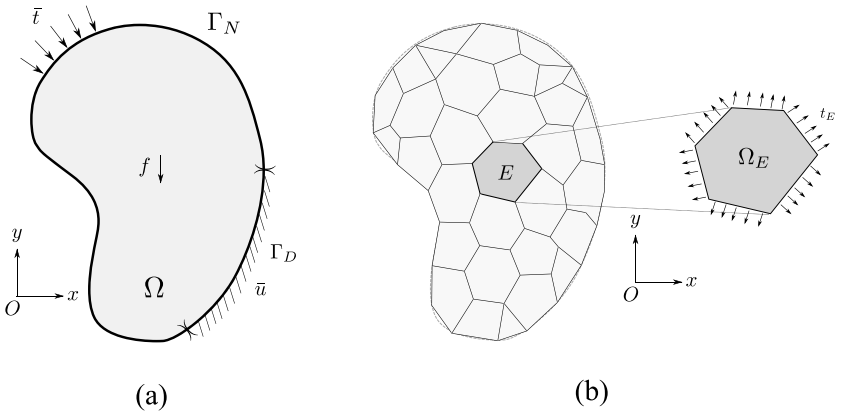

Fig. 1. (a) Physical problem in 2D, and (b) spatial discretization.

2. Formulation of the virtual element method

2.1. Governing equation

In the continuous domain, $\Omega \subset \mathbb{R}^2$, with a body force, $\boldsymbol{f}$, acting on Ω as shown in Fig. 1(a), consider the linear elastic boundary value problem. The boundary, Γ, consists of the Dirichlet boundary (Γ_D) and the Neumann boundary (Γ_N). The equilibrium equation, compatibility condition, and constitutive equation for a linear elastic material are given by

$$\boldsymbol{\partial}^{\mathrm{T}}\boldsymbol{\sigma} + \boldsymbol{f} = \boldsymbol{0} \quad \text{in } \Omega, \tag{1}$$

$$\boldsymbol{\varepsilon}(\boldsymbol{u}) = \boldsymbol{\partial}\boldsymbol{u} \quad \text{in } \Omega, \tag{2}$$

$$\boldsymbol{\sigma} = \boldsymbol{C}\boldsymbol{\varepsilon} \quad \text{in } \Omega, \tag{3}$$

where $\boldsymbol{\partial}$ is the differential operator, $\boldsymbol{u}$ is the displacement vector, $\boldsymbol{\sigma}$ is the Cauchy stress, $\boldsymbol{\varepsilon}$ is the small strain, and $\boldsymbol{C}$ is the elastic stiffness tensor. The boundary conditions are given by

$$\boldsymbol{u} = \bar{\boldsymbol{u}} \quad \text{on } \Gamma_D, \tag{4}$$

$$\boldsymbol{t} := \boldsymbol{m}\boldsymbol{\sigma} = \bar{\boldsymbol{t}} \quad \text{on } \Gamma_N, \tag{5}$$

where, $\boldsymbol{m}$ is the matrix expressed as

$$\boldsymbol{m} = \begin{bmatrix} n_x & 0 & n_y \\ 0 & n_y & n_x \end{bmatrix}. \tag{6}$$

Applying the virtual work principle, the weak form of the governing equation in terms of $\boldsymbol{u} \in \boldsymbol{\mathcal{V}}$ is given as

$$a(\boldsymbol{u}, \boldsymbol{v}) = L(\boldsymbol{v}) \quad \forall \boldsymbol{v} \in \boldsymbol{\mathcal{V}}, \tag{7}$$

where $\boldsymbol{\mathcal{V}} := \left(\mathcal{H}_0^1(\Omega)\right)^2$ is the space of admissible displacement fields, and $\boldsymbol{v}$ represents the virtual displacement belonging to $\boldsymbol{\mathcal{V}}$. Functions a and L represent the internal virtual work and the external virtual work, respectively, and are defined as follows:

$$a(\boldsymbol{u}, \boldsymbol{v}) = \int_\Omega \boldsymbol{\varepsilon}(\boldsymbol{v})^{\mathrm{T}}\boldsymbol{C}\boldsymbol{\varepsilon}(\boldsymbol{u}), \mathrm{d}\Omega \tag{8}$$

$$L(\boldsymbol{v}) = \int_\Omega \boldsymbol{v}^{\mathrm{T}}\boldsymbol{f}\,\mathrm{d}\Omega + \int_{\Gamma_N} \boldsymbol{v}^{\mathrm{T}}\bar{\boldsymbol{t}}\,\mathrm{d}\Gamma_N. \tag{9}$$

2.2. Formulation of the virtual element method

Divide domain Ω into nonoverlapping arbitrary-shaped polygons, E, as shown in Fig. 1(b). In this case, each polygon, E, is referred to as an element, and the number of edges, e, of E is denoted by m. Further, $\boldsymbol{\mathcal{V}}^h(E)$ represents the element-wise defined discretized admissible displacement field, defined as $\boldsymbol{\mathcal{V}}^h(E) = \left[\mathcal{V}^h(E)\right]^2$. Here, $\mathcal{V}^h(E)$ is a scalar space given by

$$\mathcal{V}^h(E) = \left\{ v^h \in \mathcal{H}^1(E) \mid \Delta v^h \in \mathcal{P}_{k-2}(E),\ v^h|_e \in \mathcal{P}_k(e) \quad \forall e \in \partial E \right\}, \tag{10}$$

where Δ is the Laplacian; $\mathcal{P}_{k-2}(E)$ is the space of polynomials of degree $k-2$ at most, defined on element E; and $\mathcal{P}_k(e)$ is the space of polynomials of degree k at most, defined on edge e of the element.

According to the standard formulation of the Virtual Element Method (VEM), such as that presented in Artioli et al. [14], the internal virtual work of element E can be expressed as

$$a_E\left(\boldsymbol{u}^h, \boldsymbol{v}^h\right) = a_E\left(\Pi^d \boldsymbol{u}^h, \Pi^d \boldsymbol{v}^h\right) + a_E\left(\boldsymbol{u}^h - \Pi^d \boldsymbol{u}^h, \boldsymbol{v}^h - \Pi^d \boldsymbol{v}^h\right), \tag{11}$$

where the first term on the right-hand side denotes the consistent term, the second term is the stabilization term, and $\Pi^d : \mathcal{V}^h(E) \to \mathcal{P}_k(E)$ is the projection operator. Here, because the stabilization term cannot be exactly computed, a positive definite symmetric bilinear form, $S_E(\boldsymbol{u}^h, \boldsymbol{v}^h)$, is employed for the formulation of the internal virtual work for element E. Consequently, the internal virtual work for element E is expressed as follows:

$$a_E^h\left(\boldsymbol{u}^h, \boldsymbol{v}^h\right) = a_E\left(\Pi^d \boldsymbol{u}^h, \Pi^d \boldsymbol{v}^h\right) + S_E\left(\boldsymbol{u}^h - \Pi^d \boldsymbol{u}^h, \boldsymbol{v}^h - \Pi^d \boldsymbol{v}^h\right). \tag{12}$$

2.3. Existence and uniqueness of the solution

For the solution of Eq. (7) to exist uniquely, it is required that for any $\boldsymbol{p} \in \mathcal{P}_k(E)$ and $\boldsymbol{v}^h \in \mathcal{V}^h(E)$, the following equality holds:

$$a_E^h\left(\boldsymbol{p}, \boldsymbol{v}^h\right) = a_E\left(\boldsymbol{p}, \boldsymbol{v}^h\right), \tag{13}$$

and for any $\boldsymbol{v}^h \in \mathcal{V}^h(E)$, there must exist positive constants α_* and α^*, not dependent on element E or element size h, that satisfy the following inequality:[1]

$$\alpha_* a_E\left(\boldsymbol{v}^h, \boldsymbol{v}^h\right) \le a_E^h\left(\boldsymbol{v}^h, \boldsymbol{v}^h\right) \le \alpha^* a_E\left(\boldsymbol{v}^h, \boldsymbol{v}^h\right). \tag{14}$$

The former condition is referred to as k-consistency, and the latter as stability.

For simplicity, the formulations of the consistent and stabilization terms for $k = 1$ are described. In this case, for an m-sided polygonal element, the dimension of $\mathcal{V}^h(E)$ becomes $2m$.

2.4. Formulation of the consistent term

For any function $\boldsymbol{\varepsilon}^P \in \mathcal{P}_0(E)^{2\times2}_{\mathrm{sym}}$ using the projection $\Pi^\varepsilon : \mathcal{V}^h(E) \to \mathcal{P}_0(E)^{2\times2}_{\mathrm{sym}}$ that satisfies

$$\int_{\Omega_E} \left(\boldsymbol{\varepsilon}(\boldsymbol{u}^h) - \Pi^\varepsilon(\boldsymbol{u}^h)\right)^{\mathrm{T}} \boldsymbol{\varepsilon}^P = 0, \tag{15}$$

the consistent term in Eq. (12) can be expressed as

$$a_E\left(\Pi^d \boldsymbol{u}^h, \Pi^d \boldsymbol{v}^h\right) = \int_{\Omega_E} \left[\Pi^\varepsilon(\boldsymbol{v}^h)\right]^{\mathrm{T}} \boldsymbol{C}\, \Pi^\varepsilon(\boldsymbol{u}^h) \mathrm{d}\Omega_E, \tag{16}$$

where $\Pi^\varepsilon(\boldsymbol{u}^h)$ is the best approximation of strain $\boldsymbol{\varepsilon}(\boldsymbol{u}^h)$ in the 0th-order polynomial space $\mathcal{P}_0(E)^{2\times2}_{\mathrm{sym}}$. $\Pi^\varepsilon(\boldsymbol{u}^h)$ can be represented as

$$\Pi^\varepsilon(\boldsymbol{v}^h) = \boldsymbol{N}^P \boldsymbol{\pi}^\varepsilon \tilde{\boldsymbol{v}}, \tag{17}$$

where $\tilde{\boldsymbol{v}} \in \mathbb{R}^{2m}$ is the nodal displacement vector of $\boldsymbol{v}^h \in \mathcal{V}^h(E)$ expressed in basis $\boldsymbol{N}^V$ of $\mathcal{V}^h(E)$, and $\boldsymbol{\pi}^\varepsilon \in \mathbb{R}^{3\times2m}$ is the basis transformation matrix from $\mathcal{V}^h(E)$ to $\mathcal{P}_0(E)^{2\times2}_{\mathrm{sym}}$. Since the polynomial space, $\mathcal{P}_0(E)^{2\times2}_{\mathrm{sym}}$, is a three-dimensional space represented by

$$\mathcal{P}_0(E)^{2\times2}_{\mathrm{sym}} = \mathrm{span}\left\{\begin{pmatrix}1\\0\\0\end{pmatrix}, \begin{pmatrix}0\\1\\0\end{pmatrix}, \begin{pmatrix}0\\0\\1\end{pmatrix}\right\}, \tag{18}$$

its basis, $\boldsymbol{N}^P$, is given by

$$\boldsymbol{N}^P = \begin{bmatrix}1 & 0 & 0\\ 0 & 1 & 0\\ 0 & 0 & 1\end{bmatrix}. \tag{19}$$

By substituting Eq. (17) into Eq. (15) and rearranging the equation, we obtain

$$\boldsymbol{\pi}^\varepsilon = \boldsymbol{G}^{-1}\boldsymbol{B}, \tag{20}$$

where $\boldsymbol{G}$ and $\boldsymbol{B}$ are defined as

$$\boldsymbol{G} = \int_{\Omega_E} \left(\boldsymbol{N}^P\right)^{\mathrm{T}} \boldsymbol{N}^P \mathrm{d}\Omega_E, \tag{21}$$

$$\boldsymbol{B} = \int_{\Gamma_E} \left(\boldsymbol{m}\boldsymbol{N}^P\right)^{\mathrm{T}} \boldsymbol{N}^V \mathrm{d}\Gamma_E, \tag{22}$$

respectively. Using Eqs. (20) and (17), $\Pi^\varepsilon(\boldsymbol{v}^h)$ can be expressed as

$$\Pi^\varepsilon(\boldsymbol{v}^h) = \boldsymbol{N}^P \boldsymbol{G}^{-1} \boldsymbol{B} \tilde{\boldsymbol{v}}. \tag{23}$$

Thus, the consistent term in Eq. (16) becomes

$$\int_{\Omega_E} \left[\Pi^\epsilon(\boldsymbol{v}^h)\right]^{\mathrm{T}} \boldsymbol{C}\Pi^\epsilon(\boldsymbol{u}^h)\mathrm{d}\Omega_E = (\tilde{\boldsymbol{v}})^{\mathrm{T}} \boldsymbol{K}_C \tilde{\boldsymbol{u}}, \tag{24}$$

where the stiffness matrix, $\boldsymbol{K}_C$, is given by

$$\boldsymbol{K}_C = \boldsymbol{B}^{\mathrm{T}}\boldsymbol{G}^{-\mathrm{T}}\left[\int_{\Omega_E} \left(\boldsymbol{N}^P\right)^{\mathrm{T}} \boldsymbol{C}\boldsymbol{N}^P \mathrm{d}\Omega_E\right] \boldsymbol{G}^{-1}\boldsymbol{B}. \tag{25}$$

In the process of obtaining $\boldsymbol{K}_C$ from Eq. (25), the interpolation functions, $\boldsymbol{N}^V$, of the displacement, $\boldsymbol{u}^h \in \boldsymbol{\mathcal{V}}^h(E)$, only appear in the boundary integrals of Eq. (22). Thus, in the VEM, it is sufficient to define the interpolation functions of the displacement on the element edges, and there is no need to define them within the element explicitly, hence the name, "*virtual* element method".

2.5. Formulation of the stabilization term

The formulation of the stabilization term in the second term on the right-hand side of Eq. (12) has been addressed by various methods [3,15]. In this context, we adopt a formulation based on the proposal of Artioli et al. [14].

First, we define the dimensionless element coordinates, ξ and η, using the element centroid coordinates (x_c, y_c) and the representative length of the element, h_E, as follows:

$$\xi = \frac{x - x_c}{h_E}, \quad \eta = \frac{y - y_c}{h_E}. \tag{26}$$

Subsequently, the polynomial space, $\boldsymbol{\mathcal{P}}_1(E)$, is expressed in terms of the element coordinates as follows:

$$\boldsymbol{\mathcal{P}}_1(E) = \mathrm{span}\left\{\begin{pmatrix}1\\0\end{pmatrix}, \begin{pmatrix}0\\1\end{pmatrix}, \begin{pmatrix}\xi\\0\end{pmatrix}, \begin{pmatrix}0\\\xi\end{pmatrix}, \begin{pmatrix}\eta\\0\end{pmatrix}, \begin{pmatrix}0\\\eta\end{pmatrix}\right\}. \tag{27}$$

Since the dimension of $\boldsymbol{\mathcal{P}}_1(E)$ is 6, the displacement functions, $\Pi^d\boldsymbol{u}^h$, on $\boldsymbol{\mathcal{P}}_1(E)$ can be expressed using its basis, $\boldsymbol{N}^d$, as follows:

$$\Pi^d\boldsymbol{u}^h = \boldsymbol{N}^d\hat{\boldsymbol{u}}^c. \tag{28}$$

Moreover, because $\boldsymbol{\mathcal{P}}_1(E) \subset \boldsymbol{\mathcal{V}}^h(E)$, it can also be represented using the basis, $\boldsymbol{N}^V$, of $\boldsymbol{\mathcal{V}}^h(E)$, as follows:

$$\Pi^d\boldsymbol{u}^h = \boldsymbol{N}^V\tilde{\boldsymbol{u}}^c. \tag{29}$$

Here, $\hat{\boldsymbol{u}}^c \in \mathbb{R}^6$ and $\tilde{\boldsymbol{u}}^c \in \mathbb{R}^{2m}$ are vectors representing displacement $\Pi^d\boldsymbol{u}^h$ of the consistent term in terms of bases $\boldsymbol{N}^d$ and $\boldsymbol{N}^V$, respectively. Introducing the matrix, $\boldsymbol{D} : \mathbb{R}^6 \to \mathbb{R}^{2m}$, representing the basis transformation of $\boldsymbol{\mathcal{P}}_1(E)$ into $\boldsymbol{\mathcal{V}}^h(E)$, expressed as

$$\boldsymbol{D} = \begin{bmatrix} 1 & 0 & \xi_1 & 0 & \eta_1 & 0 \\ 0 & 1 & 0 & \xi_1 & 0 & \eta_1 \\ 1 & 0 & \xi_2 & 0 & \eta_2 & 0 \\ 0 & 1 & 0 & \xi_2 & 0 & \eta_2 \\ \vdots & \vdots & \vdots & \vdots & \vdots & \vdots \\ 1 & 0 & \xi_m & 0 & \eta_m & 0 \\ 0 & 1 & 0 & \xi_m & 0 & \eta_m \end{bmatrix}, \tag{30}$$

we can express $\boldsymbol{D}\hat{\boldsymbol{u}}^c$ as

$$\boldsymbol{D}\hat{\boldsymbol{u}}^c = \tilde{\boldsymbol{u}}^c. \tag{31}$$

Therefore, $\tilde{\boldsymbol{u}}^c$ exists in $\mathrm{Im}\boldsymbol{D}$. If $m > 3$, matrix $\boldsymbol{D}$ becomes a tall full-rank matrix. In this case, the vector space, $\mathbb{R}^{2m}$, in which $\tilde{\boldsymbol{u}}$ exists can be orthogonally decomposed as follows:

$$\mathbb{R}^{2m} = \mathrm{Im}\boldsymbol{D} \oplus \mathrm{Im}\left(\boldsymbol{I} - \boldsymbol{D}\left(\boldsymbol{D}^{\mathrm{T}}\boldsymbol{D}\right)^{-1}\boldsymbol{D}^{\mathrm{T}}\right), \tag{32}$$

Here $\tilde{\boldsymbol{u}}$ is the vector representing $\boldsymbol{u}^h$ in terms of basis $\boldsymbol{N}^V$, as $\boldsymbol{u}^h = \boldsymbol{N}^V\tilde{\boldsymbol{u}} \in \boldsymbol{\mathcal{V}}^h(E)$. Furthermore, because $\tilde{\boldsymbol{u}}^c \in \mathrm{Im}\boldsymbol{D}$, the displacement vector, $\tilde{\boldsymbol{u}}^s$, of the stabilization term expressed in terms of the basis of $\boldsymbol{\mathcal{V}}^h(E)$ exists in $\mathrm{Im}(\boldsymbol{I} - \boldsymbol{D}(\boldsymbol{D}^{\mathrm{T}}\boldsymbol{D})^{-1}\boldsymbol{D}^{\mathrm{T}})$. Using this, the stiffness matrix, $\boldsymbol{K}_S$, for the stabilization term is defined as

$$\boldsymbol{K}_S := \boldsymbol{\tau}\left(\boldsymbol{I} - \boldsymbol{D}\left(\boldsymbol{D}^{\mathrm{T}}\boldsymbol{D}\right)^{-1}\boldsymbol{D}^{\mathrm{T}}\right), \tag{33}$$

and the stabilization term is defined as

$$S_E\left(\boldsymbol{u}^h - \Pi^d\boldsymbol{u}^h, \boldsymbol{v}^h - \Pi^d\boldsymbol{v}^h\right) = (\tilde{\boldsymbol{v}})^{\mathrm{T}}\boldsymbol{K}_S\tilde{\boldsymbol{u}}. \tag{34}$$

Here, for any $\boldsymbol{p} \in \boldsymbol{\mathcal{P}}_k(E)$, $\Pi^d\boldsymbol{p} = \boldsymbol{p}$ holds. Thus, for $\boldsymbol{p}$ and $\boldsymbol{v}^h$, the second term on the right-hand side of Eq. (11) becomes $a_E(\boldsymbol{p} - \Pi^d\boldsymbol{p}, \boldsymbol{v}^h - \Pi^d\boldsymbol{v}^h) = 0$. Furthermore, Eq. (34) can be rewritten as follows:

$$S_E\left(\boldsymbol{p} - \Pi^d\boldsymbol{p}, \boldsymbol{v}^h - \Pi^d\boldsymbol{v}^h\right) = (\tilde{\boldsymbol{v}})^{\mathrm{T}}\boldsymbol{\tau}\left(\boldsymbol{I} - \boldsymbol{D}\left(\boldsymbol{D}^{\mathrm{T}}\boldsymbol{D}\right)^{-1}\boldsymbol{D}^{\mathrm{T}}\right)\boldsymbol{D}\tilde{\boldsymbol{p}} = (\tilde{\boldsymbol{v}})^{\mathrm{T}}\boldsymbol{\tau}(\boldsymbol{D} - \boldsymbol{D})\tilde{\boldsymbol{p}} = 0. \tag{35}$$

From the above, it can be confirmed that the conditions of Eq. (13) are satisfied. Moreover, if $S_E(\boldsymbol{u}^h, \boldsymbol{v}^h)$ satisfies the inequalities,

$$c_0 a_E\left(\boldsymbol{v}^h, \boldsymbol{v}^h\right) \leq S_E\left(\boldsymbol{v}^h, \boldsymbol{v}^h\right) \leq c_1 a_E\left(\boldsymbol{v}^h, \boldsymbol{v}^h\right), \tag{36}$$

for positive constants c_0 and c_1 independent of the element E and the representative length, h_E, we obtain

$$\begin{aligned} a_E^h\left(\boldsymbol{v}^h, \boldsymbol{v}^h\right) &\leq a_E\left(\Pi^d \boldsymbol{v}^h, \Pi^d \boldsymbol{v}^h\right) + c_1 a_E\left(\boldsymbol{v}^h - \Pi^d \boldsymbol{v}^h, \boldsymbol{v}^h - \Pi^d \boldsymbol{v}^h\right) \\ &\leq \max\left\{1, c_1\right\}\left(a_E\left(\Pi^d \boldsymbol{v}^h, \Pi^d \boldsymbol{v}^h\right) + a_E\left(\boldsymbol{v}^h - \Pi^d \boldsymbol{v}^h, \boldsymbol{v}^h - \Pi^d \boldsymbol{v}^h\right)\right) = \alpha^* a_E\left(\boldsymbol{v}^h, \boldsymbol{v}^h\right). \end{aligned}$$

Similarly, by obtaining

$$a_E^h\left(\boldsymbol{v}^h, \boldsymbol{v}^h\right) \geq \min\left\{1, c_0\right\}\left(a_E\left(\Pi^d \boldsymbol{v}^h, \Pi^d \boldsymbol{v}^h\right) + a_E\left(\boldsymbol{v}^h - \Pi^d \boldsymbol{v}^h, \boldsymbol{v}^h - \Pi^d \boldsymbol{v}^h\right)\right) = \alpha_* a_E\left(\boldsymbol{v}^h, \boldsymbol{v}^h\right),$$

we confirm that the condition of Eq. (14) is satisfied. Thus, the solution to Eq. (7) is uniquely determined.

The quantity $\boldsymbol{\tau}$ in Eq. (33) is a scaling factor for $S_E(\cdot,\cdot)$ to satisfy the conditions in Eq. (36), which is referred to as the stabilization parameter [16]. Moreover, as discussed in Cangiani et al. [17], using the identity matrix, $\boldsymbol{I} \in \mathbb{R}^{2m\times 2m}$, the stabilization parameter is often treated as a scalar, τ, through the expression:

$$\boldsymbol{\tau} = \tau \boldsymbol{I}. \tag{37}$$

2.6. Formulation of the loading term

Consider the loading term, $L_E(\boldsymbol{v}^h)$, corresponding to a constant body force, $\boldsymbol{f} = \left\{f_x, f_y\right\}^{\mathrm{T}}$, subjected to element E. Since the interpolation functions, $\boldsymbol{N}^V$, for the virtual displacements, $\boldsymbol{v}^h$, are not explicitly defined within the element, the loading term is approximated as follows:

$$\begin{aligned} L_E(\boldsymbol{v}^h) &= \int_{\Omega_E} \left(\boldsymbol{v}^h\right)^{\mathrm{T}} \boldsymbol{f} \mathrm{d}\Omega_E \\ &\approx \left(\sum_{i=1}^{m} \frac{1}{m} (\tilde{\boldsymbol{v}})_i\right)^{\mathrm{T}} \left(\int_{\Omega_E} \boldsymbol{f} \mathrm{d}\Omega_E\right) = \tilde{\boldsymbol{v}}^{\mathrm{T}} \bar{\boldsymbol{f}}. \end{aligned} \tag{38}$$

Here, $\bar{\boldsymbol{f}}$ is a column vector of dimension $n = 2m$, which is given by

$$\bar{\boldsymbol{f}} = \frac{|\Omega_E|}{m}\left\{\begin{array}{cccccccc} f_x & f_y & f_x & f_y & \cdots & f_x & f_y \end{array}\right\}^{\mathrm{T}}. \tag{39}$$

This approximation means that each node uniformly carries the body force within the element. Notably, in the VEM, where interpolation functions are defined along the edges of the element, the formulation of the loading term corresponding to the forces subjected to the element edge is established similarly to that in the FEM.

3. Eigenvalue analysis of the element stiffness matrix

3.1. Physical meaning of the eigenvalues and eigenvectors of the element stiffness matrix

The eigenvalue analysis of the element stiffness matrix, $\boldsymbol{K}$, of the isoparametric bilinear quadrilateral element (QUAD4) affords eight independent eigenvectors, $\boldsymbol{e}_i$, along with their corresponding eigenvalues, λ_i. The eight eigenvectors correspond to the basic deformation modes of the bilinear quadrilateral element, as illustrated in Fig. 2. Furthermore, applying the eigenvector, $\boldsymbol{e}_i^{\mathrm{T}}$, from the left to the following equation of the eigenvalue problem,

$$\boldsymbol{K}\boldsymbol{e}_i = \lambda_i \boldsymbol{e}_i, \tag{40}$$

we obtain

$$\boldsymbol{e}_i^{\mathrm{T}} \boldsymbol{K} \boldsymbol{e}_i = \lambda_i \boldsymbol{e}_i^{\mathrm{T}} \boldsymbol{e}_i = \lambda_i. \tag{41}$$

The strain energy, $U(\boldsymbol{e}_i)$, stored in the element due to the deformation represented by eigenvector $\boldsymbol{e}_i$ is given by

$$U(\boldsymbol{e}_i) = \frac{1}{2} \boldsymbol{e}_i^{\mathrm{T}} \boldsymbol{K} \boldsymbol{e}_i. \tag{42}$$

Thus, the eigenvalues, λ_i, of the element stiffness matrix can be expressed as follows:

$$\lambda_i = 2U(\boldsymbol{e}_i). \tag{43}$$

This indicates that the eigenvalues are equal to two times the amount of strain energy stored in the element when it is subjected to the deformation represented by the corresponding eigenvector, $\boldsymbol{e}_i$.

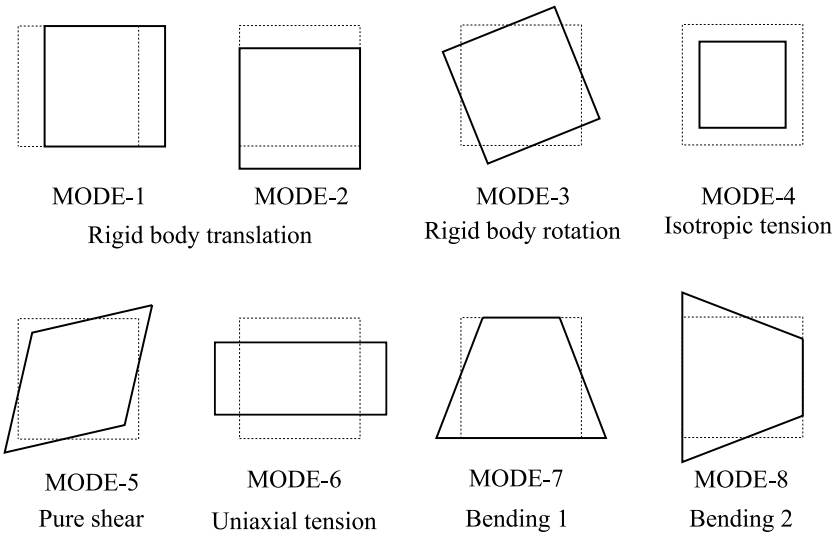

Fig. 2. Eigenmodes of the linear quadrilateral elements.

Table 1
Eigenvalues of the element stiffness matrices.

Mode	$2U$	$\boldsymbol{K}_{\mathrm{FEM}}$	$\boldsymbol{K}_{\mathrm{VEM}}$	$\boldsymbol{K}_C$	$\boldsymbol{K}_S$
4	1.923	1.923	1.923	1.923	0.000
5	0.769	0.769	0.769	0.769	0.000
6	0.769	0.769	0.769	0.769	0.000
7	0.366	0.577	1.000	0.000	1.000
8	0.366	0.577	1.000	0.000	1.000

3.2. Eigenvalues of the element stiffness matrix

Next, we consider a plane strain square element with side length 1, using Young's modulus $E = 1$ and Poisson's ratio $\nu = 0.3$. We examine the element stiffness matrix, $\boldsymbol{K}_{\mathrm{FEM}}$, of the isoparametric bilinear quadrilateral (QUAD4) element with 2×2 point complete Gauss integration in the conventional displacement-based FEM, as well as the element stiffness matrix, $\boldsymbol{K}_{\mathrm{VEM}}$, for the first-order ($k = 1$) virtual element with stabilization parameter $\tau = 1$. The eigenvalues and $2U$ values are summarized in Table 1. Here, U represents the theoretical strain energy corresponding to the basic deformation modes shown in Fig. 2.

3.2.1. Eigenvalues of the stiffness matrix of the finite element method

From Table 1, the eigenvalues of the basic deformation modes (4, 5, and 6) of QUAD4 corresponding to isotropic tension (compression), pure shear, and uniaxial tension (compression), respectively, are identical to the $2U$ values. However, the eigenvalues of the two bending modes, 7 and 8, are approximately 58% greater than the $2U$ values. This discrepancy indicates that an energy larger than the theoretical value is required to induce bending deformation in QUAD4. Solving problems with significant bending using QUAD4 elements leads to shear locking phenomena, where the element becomes excessively stiff, resulting in a loss of accuracy.

3.2.2. Eigenvalues of the stiffness matrix of the virtual element method

Similar to QUAD4, the eigenvalues corresponding to the basic deformation modes (4, 5, and 6) coincide with the $2U$ values. Conversely, the eigenvalues for the bending modes differ from the $2U$ values and the eigenvalues of QUAD4.

Since the VEM stiffness matrix, $\boldsymbol{K}_{\mathrm{VEM}}$, comprises the consistent term stiffness matrix, $\boldsymbol{K}_C$, and the stabilization term stiffness matrix, $\boldsymbol{K}_S$, as given by $\boldsymbol{K}_{\mathrm{VEM}} = \boldsymbol{K}_C + \boldsymbol{K}_S$, eigenvalue analysis is conducted separately for $\boldsymbol{K}_C$ and $\boldsymbol{K}_S$. By examining the role of each term through several analyses, the relationship between the stabilization parameter, τ, and the eigenvalues associated with the bending modes can be elucidated. The results of the eigenvalue analyses for $\boldsymbol{K}_C$ and $\boldsymbol{K}_S$, with $\tau = 1$, are shown in Table 1.

3.2.3. Eigenvalues of the consistent term

Table 1 shows that the eigenvalues of $\boldsymbol{K}_C$ for the isotropic tension (compression), pure shear, and uniaxial tension (compression) modes (4, 5, and 6) are consistent with the $2U$ values. However, the eigenvalues for the bending modes are zero, indicating that they correspond to the zero-energy mode.

Based on the formulation for the first-order element ($k = 1$) in Section 2, the consistent term is formulated to have a constant strain within the element. Consequently, it can represent the isotropic tension (compression), pure shear, and uniaxial tension (compression) modes corresponding to constant strain modes. However, it cannot represent the strain field for bending modes, where the strain distribution is linear within the element. This results in a loss of stiffness for the bending modes, similar to the reduction of the integration points to a single point in the FEM to prevent shear locking. Thus, focusing only on the consistent term results in rank deficiency, which leads to a singular stiffness matrix. Consequently, the solution cannot be obtained, or physically inappropriate deformations, such as hourglass modes, may occur.

3.2.4. Eigenvalues of the stabilization term

In this section, because $\tau = 1$, we have $\boldsymbol{K}_S = \boldsymbol{I} - \boldsymbol{D}(\boldsymbol{D}^{\mathrm{T}}\boldsymbol{D})^{-1}\boldsymbol{D}^{\mathrm{T}}$ from Eq. (33). From Table 1, it is clear that $\boldsymbol{K}_S$ has modes related to bending, and the eigenvalues corresponding to the bending modes are 1. Therefore, the stabilization term adds stiffness to the bending modes that are lost in the consistent term. Furthermore, the stabilization parameter, τ, can be interpreted as a parameter for adjusting the magnitude of the eigenvalues of the bending modes, which correspond to the strain energy.

4. Considerations on the stabilization parameter

Generally, the stabilization term is scaled by the scalar stabilization parameter, τ. However, no universally accepted method for determining the value of τ has been proposed, leaving it to the user's discretion [18].

Cangiani et al. [17] have established the connections between the stabilization term in the VEM and the hourglass control techniques in the FEM for the Poisson problem. They state that VEM can reasonably determine the appropriate setting of stabilization parameters, which is an open issue in the hourglass control finite element method. In addition, they report that while VEM is robust regarding stabilization parameters, when the stabilization parameter is too small, hourglass instability occurs. Furthermore, they mention that for vectorial problems such as elasticity, the number of spurious singular (hourglass) modes substantially increases, which likely makes it more difficult to draw direct links between the VEM and the hourglass control FEM.

In this section, methods for setting the stabilization parameter for plane stress elements within the framework of elastic problems are explored. In the numerical examples that follow in this chapter, Young's modulus is set to 1 and Poisson's ratio is set to 0 in all cases.

4.1. Existing proposal for stabilization parameters

Artioli et al. [14] employed the trace of the stiffness matrix, $\boldsymbol{K}_C$, of the consistent term to scale the element size and energy. Furthermore, based on the results of parametric studies, they proposed the value of

$$\tau = \frac{1}{2}\mathrm{tr}(\boldsymbol{K}_C), \tag{44}$$

as the stabilization parameter. However, their numerical experiments involved models with a relatively large number of elements, and it remains unclear whether this approach provides sufficient accuracy for coarse meshes.

Consider the physical meaning of expression (44). As discussed in the previous section, $\boldsymbol{K}_C$ involves the modes corresponding to isotropic tension (compression), pure shear, and uniaxial tension (compression), and its eigenvalues for the other modes are zero. Therefore, $\mathrm{tr}(\boldsymbol{K}_C)$ can be expressed as

$$\mathrm{tr}(\boldsymbol{K}_C) = \lambda_4 + \lambda_5 + \lambda_6, \tag{45}$$

where λ_4, λ_5, and λ_6 are the eigenvalues corresponding to the isotropic tension (compression), pure shear, and uniaxial tension (compression) modes, respectively. Furthermore, since the value of the stabilization parameter, τ, for the first-order element is two times the magnitude of the strain energy for the bending modes, Eq. (44) can be expressed as follows:

$$U(\boldsymbol{e}_7) = \frac{1}{2}\left\{U(\boldsymbol{e}_4) + U(\boldsymbol{e}_5) + U(\boldsymbol{e}_6)\right\}. \tag{46}$$

The above equation shows that Eq. (44) assigns the magnitude of the strain energy for bending as half of the total strain energy for isotropic tension (compression), pure shear, and uniaxial tension (compression).

In addition, Reddy and Huyssteen [19] suggested defining the stabilization parameter using Lamé's second constant, μ, as

$$\tau = \mu. \tag{47}$$

Since the theoretical value, λ_5, for the pure shear mode shown in Fig. 2 is given by $\lambda_5 = 2\mu$, from Eq. (47), we obtain

$$U(\boldsymbol{e}_7) = \frac{1}{2}U(\boldsymbol{e}_5). \tag{48}$$

Therefore, it can be understood that Eq. (47) determines the magnitude of the strain energy for the bending mode as half of the strain energy for the shear mode.

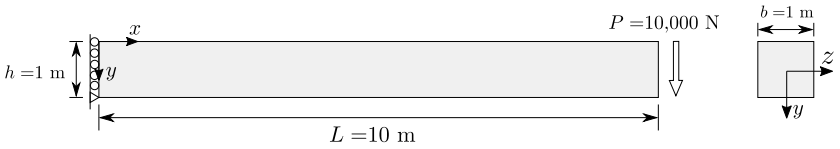

Fig. 3. A beam subjected to shear–bending.

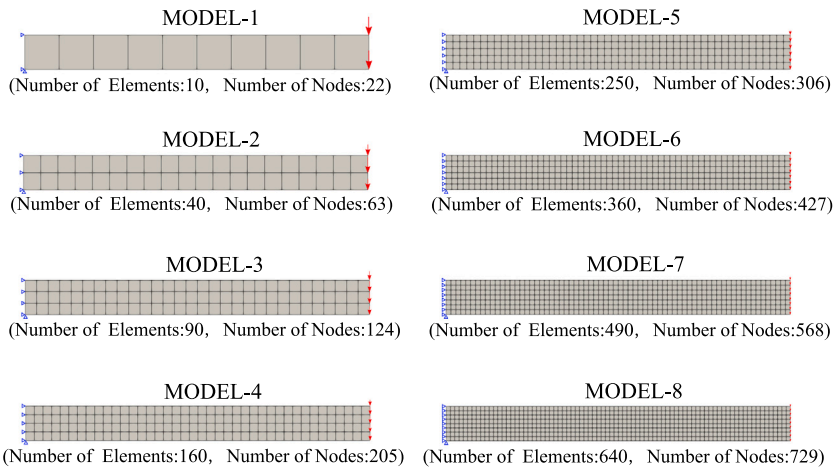

Fig. 4. Models for the shear–bending problem.

Table 2
Normalized eigenvalues corresponding to the bending modes for each element.

VEM-1	VEM-2	VEM-3	QUAD4
1.0	4.5	1.5	1.5

4.2. Stabilization parameters based on the strain energy density

Numerical tests were conducted for the shear–bending problem of the cantilever beam shown in Fig. 3 using eight models. The domain was divided into square elements, as shown in Fig. 4. The number of divisions for model i ($i = 1, 2, \ldots, 8$) was set to $10i$ and i in the x and y directions, respectively. Distributed loads were applied to the free edges of the elements. The elements employed included VEM elements with $\tau = E/3$ corresponding to two times the bending strain energy density for the stabilization parameter (τ; VEM-1), VEM elements with τ defined by Eq. (44) (VEM-2), VEM elements with τ defined by Eq. (47) (VEM-3), and QUAD4 elements as FEM elements. The eigenvalues corresponding to the bending modes for each element are shown in Table 2. The eigenvalues are normalized by two times the theoretical value of the strain energy corresponding to the bending modes. Fig. 5 shows the relationship between the maximum displacement in the y direction obtained for each model and the number of nodes in the model. The maximum displacement is normalized with respect to the solution based on the Timoshenko beam theory.

Examining the results of VEM-1, it is evident that even a model with the fewest nodes can produce solutions with an error of less than 1% when compared with the analytical solution. This result shows that a proper representation of the bending deformation can be achieved by setting the stabilization parameter corresponding to the eigenvalue of the bending mode to the theoretical strain energy value.

The results produced by VEM-3 are identical to those of QUAD4. This is because the value of μ set for τ matches the eigenvalues associated with the bending mode in QUAD4, as shown in Table 2. In addition, the elements become rigid against bending because the value of τ is larger than the theoretical value. In this case, when there are fewer divisions, the displacement is evaluated as being smaller than the analytical solution.

Finally, among the elements examined, VEM-2 produced the least accurate results. As shown in Table 2, this is because the value of τ set in VEM-2 is three times that in VEM-3 and 4.5 times that in VEM-1. Thus, VEM-2 becomes the stiffest element against bending compared with other elements, accounting for such results.

The relationship between the number of degrees of freedom in the model and the relative error of the numerical solutions to the analytical solution is shown in Fig. 6. From this figure, it can be confirmed that the convergence rate of the analysis error when increasing the number of degrees of freedom is approximately 1.0 for all models.

These findings indicate that the analysis accuracy may deteriorate if the conventional method for determining the stabilization parameter is applied to bending-dominated problems. Conversely, by defining the stabilization parameters based on the theoretical value of the bending strain energy, these types of problems can also be accurately solved.

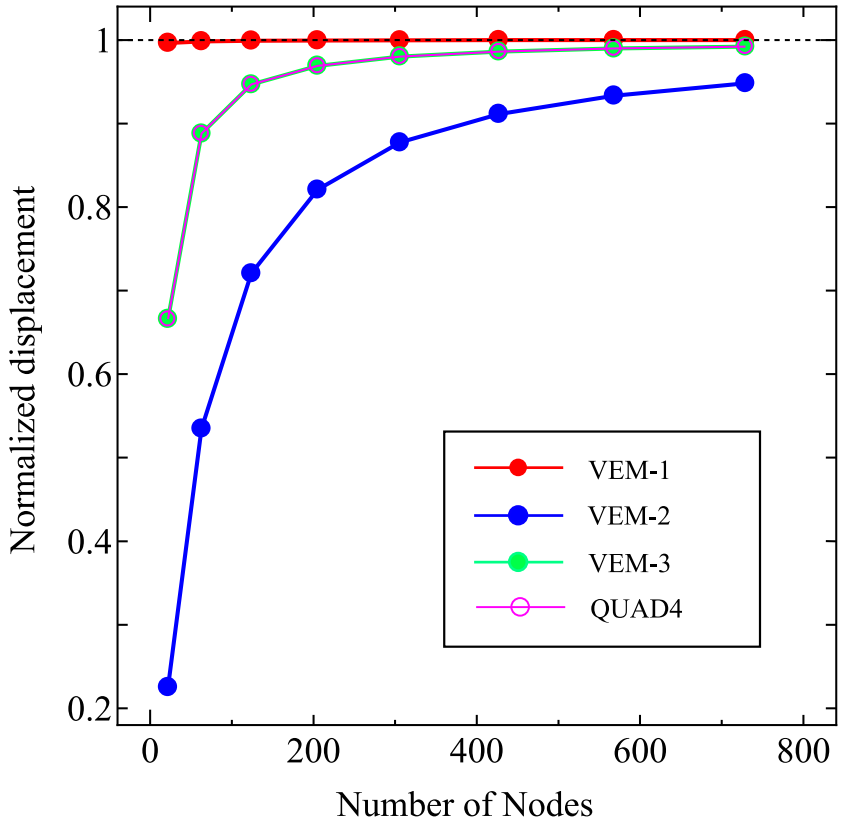

Fig. 5. Numerical results for the shear–bending problem.

Table 3
Normalized displacement at the center of the span for each case.

Model	1	2	3	4
Case 1	0.740	0.972	0.995	1.004
Case 2	0.047	0.145	0.393	0.714
Case 3	0.740	0.959	0.983	0.992
Proposed	0.740	0.924	0.983	0.992

4.3. Stabilization parameters considering the direction for elements with large aspect ratios

Consider the simple beam problem shown in Fig. 7 using a model that divides the elements, as shown in Fig. 8 with rectangular elements having an aspect ratio of 10. The number of divisions for model i (where $i = 1, 2, 3, 4$) is $2i$ in both the x and y directions. A concentrated load is applied to the top node in the center of the span.

Given the results of the previous section, we start with Case 1, where the stabilization parameter is defined as $\tau = \frac{E}{3}\frac{h_y}{h_x}$, a value based on the strain energy density of mode 7 in Fig. 2.

Table 3 shows the relationship between the number of nodes in each model and the maximum displacement in the middle of the span obtained in Case 1, normalized by the reference solution. The reference solution uses the result of the FEM with 25,000 QUAD4 elements, consisting of 500 elements in the x-direction and 50 elements in the y-direction.

The deformation of the simple beam by model 2 with 16 elements is shown in Fig. 9. The accuracy of the solution for Case 1, as shown in Table 3, is good. However, Fig. 9 shows the occurrence of physically inappropriate deformation where the normal strain, ϵ_y, in the y direction oscillates. The cause of this issue is as follows: for rectangular elements, the strain energies required to generate bending modes 1 and 2 (as shown in Fig. 2) are different. However, an incorrect energy value was assigned to bending mode 2 because the energy value related to bending mode 1 was assigned to the stabilization parameter. In this numerical example, the aspect ratio of the elements is 10. Consequently, the theoretical strain energy required for bending mode 2 is 100 times greater than that required for bending mode 1. This underestimation of the stiffness of bending mode 2 to 1/100 of the theoretical value results in inappropriate deformation.

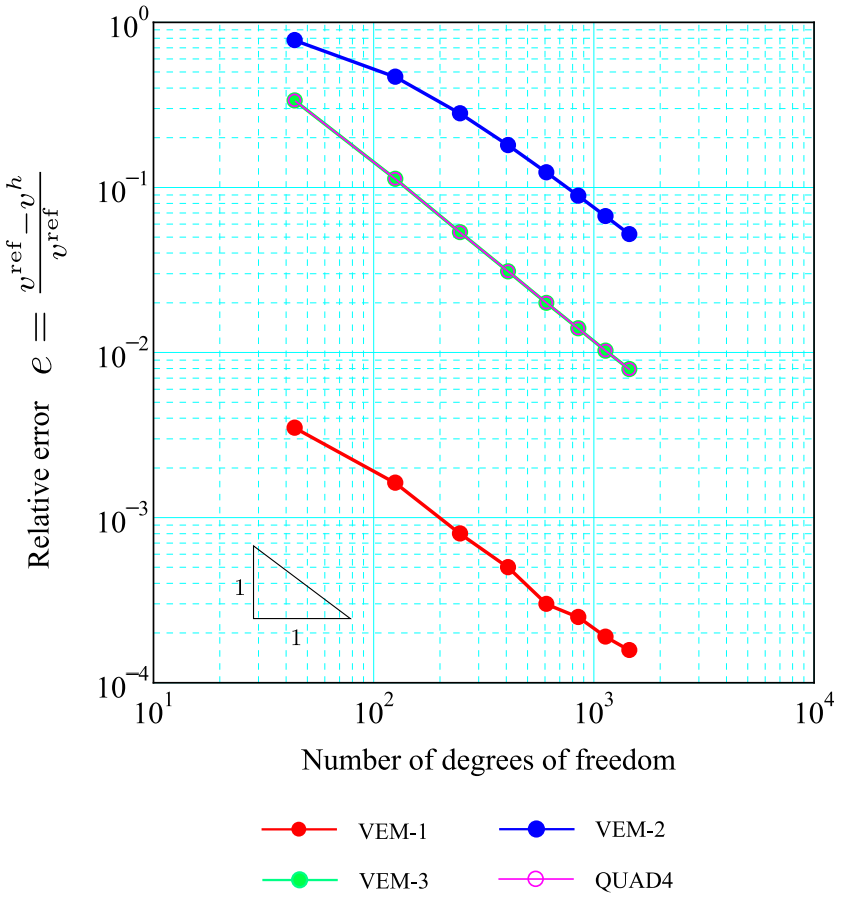

Fig. 6. Number of degrees of freedom and error for each element.

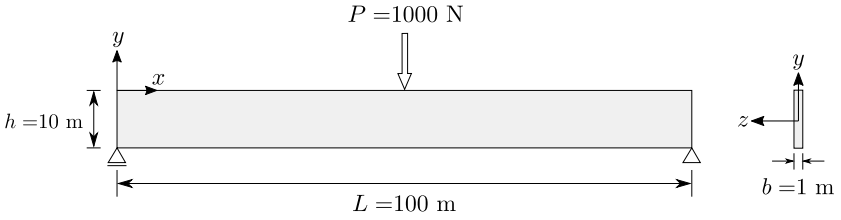

Fig. 7. Simple beam subjected to a concentrated load at the center of the span.

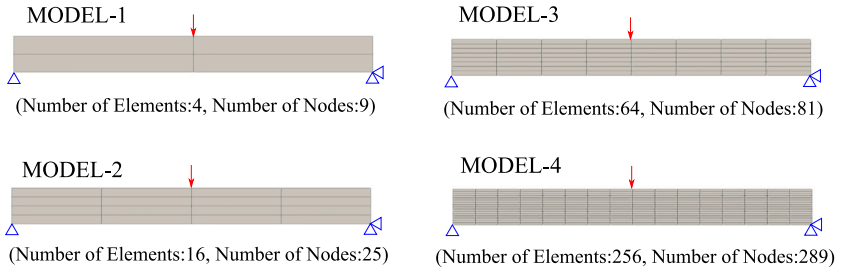

Fig. 8. Models for the simple beam.

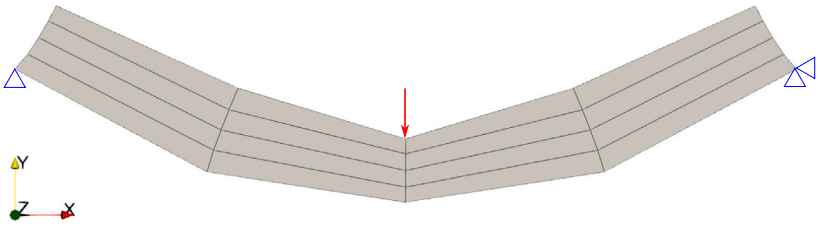

Fig. 9. Deformation of Model 2 in Case 1.

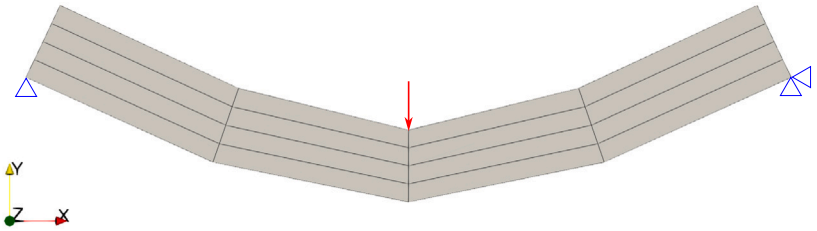

Fig. 10. Deformation of Model 2 in Case 2.

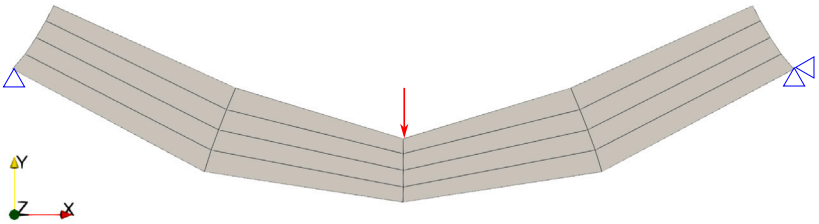

Fig. 11. Deformation of Model 2 in Case 3.

Next, we analyzed Cases 2 and 3. In Case 2, the stabilization parameter was given as $\tau = \frac{E}{3}\frac{h_x}{h_y}$, based on the theoretical strain energy density related to bending mode 2. In Case 3, the stabilization parameter was given as $\tau = \frac{E}{3}$, which is the average of Cases 1 and 2. The normalized maximum displacement at the center of the span obtained in each case is shown in Table 3. The deformations by Model 2 in Cases 2 and 3 are shown in Figs. 10 and 11, respectively. From these results, it is evident that for Case 2, although no inappropriate deformation occurs as in Case 1, the accuracy of the solution obtained is low. This is because the stiffness of bending mode 1 is overestimated by 100 times the theoretical value by setting the strain energy of bending mode 1 equal to that of bending mode 2. In Case 3, the analysis accuracy is comparable to that in Case 1. However, it has been confirmed that inappropriate deformation of the elements occurs, as in Case 1.

4.4. Proposal of the stabilization parameter considering the direction

The abovementioned problem cannot be solved if the stabilization parameter is represented as a scalar. As a solution, we propose an approach that involves representing the stabilization parameter as a diagonal matrix containing directional information instead of a scalar. The stabilization parameter is defined using two parameters: $\tau_1 = \frac{E}{3}\frac{h_y}{h_x}$, which is based on the strain energy density for mode 7, and $\tau_2 = \frac{E}{3}\frac{h_x}{h_y}$, which is based on the strain energy density for mode 8. Since the rectangular element in this study has

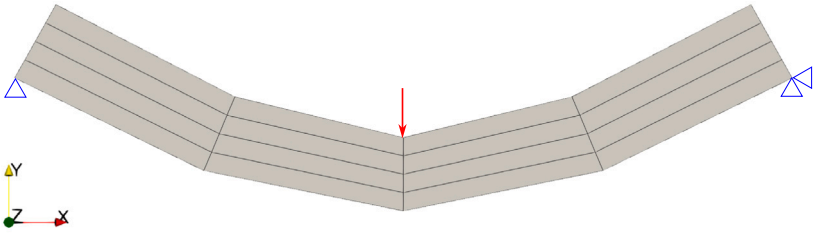

Fig. 12. Deformation of Model 2 for the proposed method.

eight degrees of freedom, the stabilization parameter, $\boldsymbol{\tau}$, can be expressed as follows:

$$\boldsymbol{\tau} = \begin{bmatrix} \tau_1 & & & & & & & \\ & \tau_2 & & & & & & \\ & & \tau_1 & & & & & \\ & & & \tau_2 & & & & \\ & & & & \tau_1 & & & \\ & & & & & \tau_2 & & \\ & & & & & & \tau_1 & \\ & & & & & & & \tau_2 \end{bmatrix}. \tag{49}$$

The condition that guarantees the stability of the solution is that the stiffness matrix corresponding to the proposed stabilization parameter, $\boldsymbol{\tau}$, is a positive definite symmetric matrix [17]. Since the matrix in Eq. 49 is symmetric and all its eigenvalues are positive, it becomes a positive definite matrix, thus satisfying the stability condition. Using the proposed stabilization parameter, the normalized maximum displacements obtained in each model when solving the problem shown in Fig. 7 are shown in Table 3, and the deformation of Model 2 is shown in Fig. 12. The results confirm that the stabilization parameter in Eq. 49 yields a more accurate solution than that obtained in Case 2, without inducing inappropriate deformation of the elements, as in Case 1 and Case 3.

In this section, we deliberated on the method for setting the stabilization parameter, a process yet to be established. By considering the strain energy density for the deformation mode, expressed through the stabilization term, along with the directional information, we demonstrated that precise analysis can be accomplished even for elements with a high aspect ratio.

Using stabilization terms that consider aspect ratio has been shown to be advantageous for rectangular elements with large aspect ratio. Although numerical experiments on general polygons are not carried out in this paper, it is possible to determine the smallest ellipse enclosing any polygon. By establishing a local coordinate system along the principal axis of the ellipse, one can devise stabilization terms based on the lengths of the principal and minor axes in this local coordinate system using the proposed method.

5. Concluding remarks

This study clarifies the roles of the consistent and stabilization terms, both of which are integral to the internal virtual work in the VEM. To this end, we conducted a series of eigenvalue analyses of plane elements. Drawing on these results, we proposed a method for defining the stabilization parameters, enabling accurate analysis irrespective of the element's aspect ratio.

- The stabilization term of the first-order quadrilateral element introduces bending modes. The value of the stabilization parameter corresponds to the eigenvalue of the bending modes.
- Setting the stabilization parameters based on the bending strain energy density results in a more accurate solution compared with that obtained with the previously proposed method.
- When using a scalar stabilization parameter for elements with large aspect ratios, inappropriate deformation may occur. This problem can be resolved by providing directional information to the stabilization parameters.

This study presents a basic investigation of the element characteristics using bilinear quadrilateral elements. Moreover, the VEM can handle not only quadrilaterals but also arbitrary polygons, including nonconvex shapes. Therefore, future studies should focus on extending this method to arbitrarily shaped elements.

CRediT authorship contribution statement

Ryuta Fujimoto: Writing – review & editing, Writing – original draft, Visualization, Investigation. **Isao Saiki:** Writing – review & editing, Writing – original draft, Validation, Supervision, Resources.

Declaration of competing interest

The authors declare that they have no known competing financial interests or personal relationships that could have appeared to influence the work reported in this paper.

Data availability

No data was used for the research described in the article.

References

[1] L. Beirão Da Veiga, F. Brezzi, A. Cangiani, G. Manzini, L.D. Marini, A. Russo, Basic principles of virtual element methods, Math. Models Methods Appl. Sci. 23 (1) (2013) 199–214.
[2] L. Beirão Da Veiga, F. Brezzi, L.D. Marini, Virtual elements for linear elasticity problems, SIAM J. Numer. Anal. 51 (2) (2013) 794–812.
[3] A.L. Gain, C. Talischi, G.H. Paulino, On the virtual element method for three-dimensional linear elasticity problems on arbitrary polyhedral meshes, Comput. Methods Appl. Mech. Engrg. 282 (2014) 132–160.
[4] H. Chi, L. Beirão Da Veiga, G.H. Paulino, Some basic formulations of the virtual element method (VEM) for finite deformations, Comput. Methods Appl. Mech. Engrg. 318 (2017) 148–192.
[5] E. Artioli, L. Beirão Da Veiga, C. Lovadina, E. Sacco, Arbitrary order 2D virtual elements for polygonal meshes: Part II, inelastic problem, Comput. Mech. 60 (2017) 643–657.
[6] P.F. Antonietti, M. Bruggi, S. Scacchi, M. Verani, On the virtual element method for topology optimization on polygonal meshes: A numerical study, Comput. Math. Appl. 74 (5) (2017) 1091–1109.
[7] P. Wriggers, W.T. Rust, B.D. Reddy, A virtual element method for contact, Comput. Mech. 58 (6) (2016) 1039–1050.
[8] M.F. Benedetto, A. Caggiano, G. Etse, Virtual elements and zero thickness interface-based approach for fracture analysis of heterogeneous materials, Comput. Methods Appl. Mech. Engrg. 338 (2018) 41–67.
[9] L. Beirão Da Veiga, C. Lovadina, A. Russo, Stability analysis for virtual element methods, Math. Models Methods Appl. Sci. 27 (13) (2017) 2557–2594.
[10] L. Chen, J. Huang, Some error analysis on virtual element methods, Calcolo 55 (1) (2018) 1–23.
[11] S.C. Brenner, Q. Guan, L.Y. Sung, Some estimates for virtual element methods, Comput. Methods Appl. Math. 17 (4) (2017) 553–574.
[12] S.C. Brenner, L.Y. Sung, Virtual element methods on meshes with small edges or faces, Math. Models Methods Appl. Sci. 28 (7) (2018) 1291–1336.
[13] L. Mascotto, The role of stabilization in the virtual element method: A survey, Comput. Math. Appl. 151 (2023) 244–251.
[14] E. Artioli, L. Beirão Da Veiga, C. Lovadina, E. Sacco, Arbitrary order 2D virtual elements for polygonal meshes: Part I, elastic problem, Comput. Mech. 60 (3) (2017) 355–377.
[15] L. Beirão Da Veiga, C. Lovadina, D. Mora, A virtual element method for elastic and inelastic problems on polytope meshes, Comput. Methods Appl. Mech. Engrg. 295 (2015) 327–346.
[16] L. Beirão Da Veiga, F. Brezzi, L.D. Marini, A. Russo, The Hitchhiker's guide to the virtual element method, Math. Models Methods Appl. Sci. 24 (8) (2014) 1541–1573.
[17] A. Cangiani, G. Manzini, A. Russo, N. Sukumar, Hourglass stabilization and the virtual element method, Internat. J. Numer. Methods Engrg. 102 (3–4) (2015) 404–436.
[18] M. Mengolini, M.F. Benedetto, A.M. Aragón, An engineering perspective to the virtual element method and its interplay with the standard finite element method, Comput. Methods Appl. Mech. Engrg. 350 (2019) 995–1023.
[19] B.D. Reddy, D. Huyssteen, A virtual element method for transversely isotropic elasticity, Comput. Mech. 64 (2019) 971–988.